

05,04

Magnetoelectric properties of samarium iron garnet

© D.I. Plokhov^{1,2}, A.I. Popov³, A.K. Zvezdin^{1,4}

¹ Prokhorov Institute of General Physics, Russian Academy of Sciences, Moscow, Russia

² Russian Peoples — Friendship University, Moscow, Russia

³ National Research University of Electronic Technology (MIET), Zelenograd, Russia

⁴ Lebedev Physical Institute Lebedeva RAS, Moscow, Russia

E-mail: dmitry.plokhov@gmail.com, zvezdin@gmail.com

Received December 29, 2022

Revised December 30, 2022

Accepted December 30, 2022

The magnetoelectricity of samarium iron garnet is theoretically investigated: the antiferroelectric structures of samarium ions are described and their connection with the configurations of the magnetic moments of the ions and their transformations during magnetic phase transitions is revealed. The possibility of the appearance at low temperatures of unusual Bloch domain walls, in which the magnetization vector rotates from the $[uv0]$ axes to the $[vu0]$ axes, which are not crystal symmetry axes, is established. The electric polarization of Bloch domain walls, which are realized both at low ($T \rightarrow 0$ K) and high temperatures, is studied. It has been established that the electric polarization of Bloch boundaries, which arises because of an inhomogeneous magnetoelectric effect, depends significantly on their shape.

Keywords: rare-earth iron garnets, magnetic phase transitions, Bloch domain walls, inhomogeneous magnetoelectric effect.

DOI: 10.21883/PSS.2023.03.55584.561

1. Introduction

At present, intensive research is being carried out on materials with magnetoelectric properties [1,2]. In most cases (bismuth ferrite, ferrobates, manganites) the occurrence of magnetoelectric effects of materials is due to the presence of odd magnetic configurations of d -ions (Fe, Mn, Cr) included in their composition.

In recent years, interest has increased in the study of rare-earth (RE) magnetoelectrics, whose properties are formed due to the interaction of magnetic sublattices formed by rare-earth f -ions and d -iron ions [3]. Rare-earth ferrites with a garnet structure (REFG) [4,5] belong to a new class of such magnetoelectrics. In work [5] it was shown that in rare-earth garnets the magnetic field, in particular, the field of the exchange R-Fe interaction, as well as the field of elastic stresses [6], leads to the appearance of electric dipole moments for RE-ions. The set of electric dipole moments of the subsystem of RE-ions in garnet crystals form (in case of uniform magnetic fields) complex antiferroelectric structures with zero resulting polarization, closely related to magnetic structures.

In case of an inhomogeneous magnetic field, which is realized, for example, in the zone of domain walls, „decompensation“ of electric dipole moments of RE-ions occurs, which leads to the appearance of electric polarization of the RE-subsystem ions in the region of a heterogeneous field [5].

This circumstance is determined not by the point, but by the spatial symmetry of the crystal [6], in connection with which one should clearly distinguish between the primitive and lattice cells of the crystal. We note that in work [5] the electric dipole moment of the primitive cell doubled as the polarization of the domain walls was taken, while in such cases the lattice cell [6] should be used.

In the present work, we study the magnetoelectric properties of rare-earth samarium iron garnet $\text{Sm}_3\text{Fe}_5\text{O}_{12}$ (SmIG — Samarium Iron Garnet). The choice of this material as an object of study is due to the following circumstances: firstly, Sm^{3+} ions are part of the iron garnet films used in practice, and secondly, the characteristics of SmIG, such as, for example, the anisotropy energy, the magnetization of the RE- sublattice, and others, decrease with increasing temperature not as rapidly as in the case of the rest (except for Eu^{3+}) RE-ions, and have significant even at room temperature.

At low temperatures, SmIG also has unique magnetic properties [7–9], which include the existence of spontaneous orientational phase transitions $[uv0] \leftrightarrow [110]$ at a temperature of 18 K and $[110] \leftrightarrow [111]$ at a temperature of 65.7 K, which will be considered in detail below.

In this work, we study the antiferroelectric structures of Sm^{3+} ions depending on the configurations of their magnetic moments, which are realized during magnetic phase transitions. The polarizations of domain walls that

arise in the limit of low temperatures (a Bloch wall in which the magnetization vector rotates from the easy magnetization axis $[210]$ to the easy magnetization axis $[120]$) are studied, while the polarization \mathbf{P} of the wall is directed along the axis of rotation $[001]$ and the walls, which are realized at high temperatures, when the magnetization is rotated away from the direction $[111]$ to the direction $[11\bar{1}]$ along the axis $\tilde{z} \parallel [\bar{1}10]$ (in this case, the polarization \mathbf{P} is oriented perpendicular to the axis of rotation $[\bar{1}10]$).

2. Crystal structure of ferrite garnets

Rare-earth crystals with a garnet structure have a number of unique magnetic, magnetic elastic, and magneto-optical properties, due in most cases to the presence of RE-ions in their composition. They have the general chemical formula $R_3M_5O_{12}$, where R is a rare earth element or yttrium and M is a metal. Such compounds have a very complex crystallographic structure, which is described by the spatial group $O_h^{10} - Ia\bar{3}d$. The lattice cell is body-centered cubic and includes eight formula units $R_3M_5O_{12}$, i.e. contains 160 atoms. The cell edge length is 1.2 nm.

The fact that RE-ions in garnet crystals are located in six non-equivalent c -positions is of great importance, the symmetry of the environment of which is not cubic, but is described by the D_2 point group, which does not contain spatial inversion operations (which is fundamentally important for understanding the magneto electric properties of garnets [4]). The coordinates of all 24 c -positions of RE-ions and the orientations of the symmetry axes of the first six places are given in the table. The numbering of places of RE-ions in the cell is chosen such that the environment of the place with number $k+6$ differs from the environment of the k -th place by the inversion operation, i.e., $\mathbf{e}_\alpha^{(k+6)} = -\mathbf{e}_\alpha^{(k)}$. Iron ions in rare-earth ferrite garnets are distributed over two sublattices, one of which — a -sublattice — is formed by Fe^{3+} ions at sites with an

Coordinates of c -positions (in units of cell edge length) and orientation of symmetry axes of c -positions.

k	1	2	3	4	5	6
$\mathbf{e}_x^{(k)}$	110	$1\bar{1}0$	011	$01\bar{1}$	101	$\bar{1}01$
$\mathbf{e}_y^{(k)}$	$\bar{1}10$	110	$0\bar{1}1$	011	$10\bar{1}$	101
$\mathbf{e}_z^{(k)}$	001	001	100	100	010	010
$\mathbf{r}^{(k)}$	$0\frac{3}{4}\frac{3}{8}$	$0\frac{1}{4}\frac{1}{8}$	$\frac{3}{8}0\frac{3}{4}$	$\frac{1}{8}0\frac{1}{4}$	$\frac{3}{4}\frac{3}{8}0$	$\frac{1}{4}\frac{1}{8}0$
$\mathbf{r}^{(k+6)}$	$0\frac{1}{4}\frac{5}{8}$	$0\frac{3}{4}\frac{7}{8}$	$\frac{5}{8}0\frac{1}{4}$	$\frac{7}{8}0\frac{3}{4}$	$\frac{1}{4}\frac{5}{8}0$	$\frac{3}{4}\frac{7}{8}0$
$\mathbf{r}^{(k+12)}$	$\frac{1}{2}\frac{1}{4}\frac{7}{8}$	$\frac{1}{2}\frac{3}{4}\frac{5}{8}$	$\frac{7}{8}\frac{1}{2}\frac{1}{4}$	$\frac{5}{8}\frac{1}{2}\frac{3}{4}$	$\frac{1}{4}\frac{7}{8}\frac{1}{2}$	$\frac{3}{4}\frac{5}{8}\frac{1}{2}$
$\mathbf{r}^{(k+18)}$	$\frac{1}{2}\frac{3}{4}\frac{1}{8}$	$\frac{1}{2}\frac{1}{4}\frac{3}{8}$	$\frac{1}{8}\frac{1}{2}\frac{3}{4}$	$\frac{3}{8}\frac{1}{2}\frac{1}{4}$	$\frac{3}{4}\frac{1}{8}\frac{1}{2}$	$\frac{1}{4}\frac{3}{8}\frac{1}{2}$

octahedral environment, the second — d -sublattice — Fe^{3+} ions in places with a tetrahedral environment.

3. Magnetic structures and orientational phase transitions

In rare-earth iron garnets, the ordering of the magnetic moments of rare-earth ions is carried out mainly due to the negative exchange interaction of RE-ions with Fe^{3+} iron ions in d -sublattice, and the effective interaction field R-Fe is $H_{\text{eff}} = \lambda M_d \sim 10$ T. The exchange interaction between the RE-ions themselves is an order of magnitude smaller than the exchange R-Fe interaction, and therefore will not be taken into account below. In turn, the interaction of RE-ions with the crystal field in ferrite-garnet crystals is much larger than the exchange R-Fe interaction.

In samarium ferrite garnet at temperatures $T_1 = 65.7$ K and $T_2 = 18$ K spontaneous orientational phase transitions [7,8] are observed. At the temperature $T > T_1$, the SmIG magnetization is oriented along axes of the $[111]$ type, in the interval $T_2 < T < T_1$ it is directed along $[110]$, and finally, at $T < T_2$ the crystal magnetization deviates from the $[110]$ axis in the (001) plane, and the $[uv0]$ phase is realized. The transition $[111] \leftrightarrow [110]$ is a phase transition of the first kind, while the transition $[110] \leftrightarrow [uv0]$ is a second-order phase transition. The reason for these phase transitions lies in the features of the splitting of the levels of Sm^{3+} ions in the crystal field and the field of the exchange R-Fe interaction [10].

The main multiplet of the samarium ion Sm^{3+} is the multiplet ${}^6H_{5/2}$, which in the crystal field splits into three doublets, which, according to [10], have energies $E_0 = 0 \text{ cm}^{-1}$, $E_1 = 76 \text{ cm}^{-1}$ and $E_2 = 313 \text{ cm}^{-1}$. The main doublet differs by the strong anisotropy of the g -tensor: $g_x \gg g_y, g_z$ in the local axes (see table). Let us neglect the values g_y and g_z . In this case, the level splitting of the ground doublet in the exchange field $\mathbf{H}_{\text{eff}} = \lambda \mathbf{M}_{\text{Fe}}$

$$\begin{aligned} E_{1,2}^{(k)} &= \pm \mu_B g_x (\mathbf{H}_{\text{eff}} \cdot \mathbf{e}_x^{(k)}) = \pm \mu_x (\mathbf{H}_{\text{eff}} \cdot \mathbf{e}_x^{(k)}) \\ &= \pm \mu_x \lambda M_{\text{Fe}} (\mathbf{m} \cdot \mathbf{e}_x^{(k)}), \end{aligned} \quad (1)$$

where $\mu_x = g_x \mu_B$ and $\mathbf{m} = \mathbf{M}_{\text{Fe}} / M_{\text{Fe}}$. The magnetic moment of the samarium ion Sm^{3+} , due to the splitting in the level field of the ground doublet, is collinear to the local x -axis

$$M_x^{(k)} = \mu_x \text{th} \left(\frac{\mu_x \lambda M_{\text{Fe}} (\mathbf{m} \cdot \mathbf{e}_x^{(k)})}{kT} \right). \quad (2)$$

In general terms, orientational phase transitions in SmIG were studied in works [7,8], where it was shown that they are manifestations of the magnetic analogue of the Jahn–Teller effect [11]. The theoretical description of the transitions was carried out on the basis of an analysis of the

extreme properties of the thermodynamic potential

$$\Phi = -K_1(m_x^4 + m_y^4 + m_z^4) - \frac{kT}{6} \sum_{k=1}^6 \ln \operatorname{ch} \left(\frac{\mu_x \lambda M_{\text{Fe}} (\mathbf{m} \cdot \mathbf{e}_x^{(k)})}{kT} \right), \quad (3)$$

where K_1 — is the magnetic anisotropy constant.

Expression (3) is written taking into account the levels of only the ground doublet of Sm^{3+} ions, which is valid at temperatures $T < T^* = E_1/k \sim 120$ K. The first term in relation (3) is the anisotropy energy of iron ions and the contribution of the Van Vleck type from the overlying levels of samarium ions. Let us note that the anisotropy constant K_1 depends weakly on temperature.

At low temperatures $T \rightarrow 0$ K expression (3) takes the form

$$\Phi = -K_1(m_x^4 + m_y^4 + m_z^4) - \frac{\mu_x H_{\text{eff}}}{6} \sum_{k=1}^6 |\mathbf{m} \cdot \mathbf{e}_x^{(k)}|. \quad (4)$$

The main contribution to the thermodynamic potential Φ comes from the second term, which can be completely

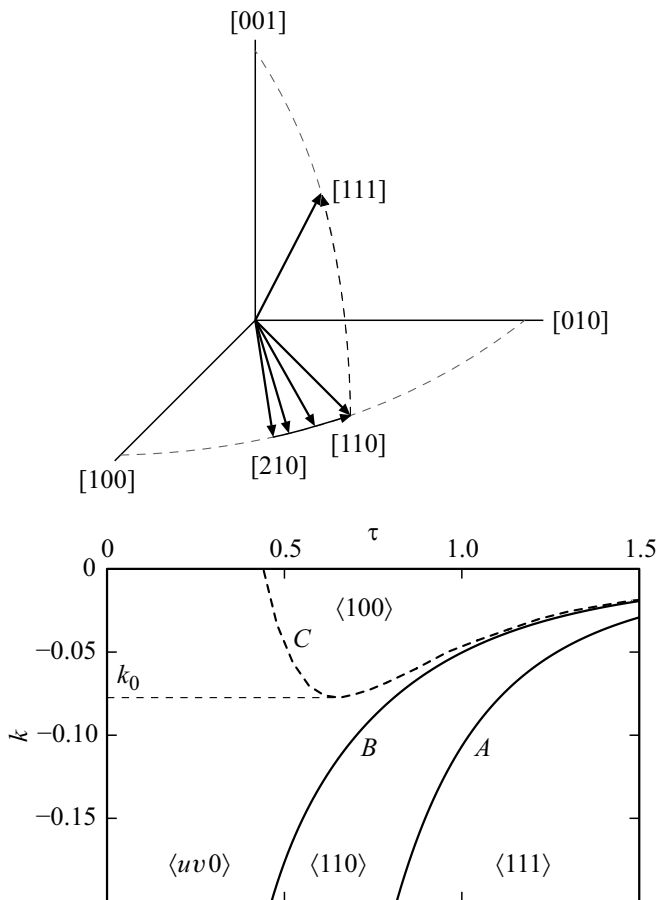


Figure 1. *a* — is a direction of the magnetization vector \mathbf{M}_{Fe} of the iron sublattice in various magnetic phases of samarium iron garnet. *b* — is a magnetic phase diagram of the crystal in the variables $\tau = T/(\mu_x \lambda M_{\text{Fe}})$ and $k = 2K_1/(\mu_x \lambda M_{\text{Fe}})$.

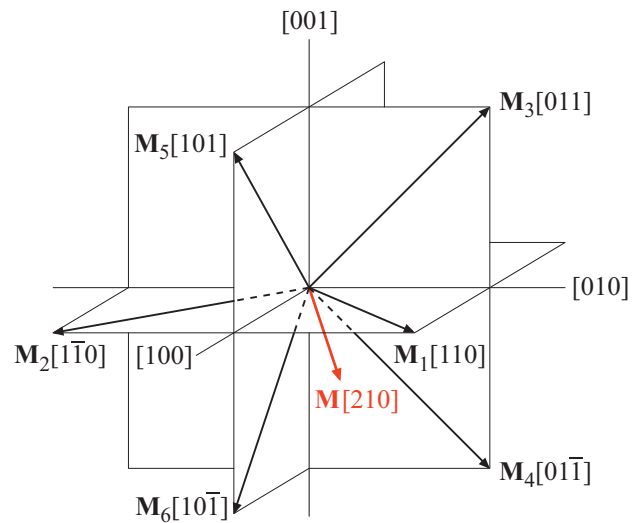


Figure 2. Configuration of magnetic moments of samarium ions in the $[210]$ phase, which is realized at $T \rightarrow 0$ K. The magnetic moments \mathbf{M}_1 and \mathbf{M}_2 lie in the plane (001) , the magnetic moments \mathbf{M}_3 and \mathbf{M}_4 lie in the (100) plane, the magnetic moments \mathbf{M}_5 and \mathbf{M}_6 lie in the (010) plane. At a finite temperature, the magnetization \mathbf{M} slightly deviates from $[210]$ to $[110]$.

taken into account in expression (4) in the first approximation. In this case, the easy magnetization axes of SmIG are directions of the $[210]$ type, which do not coincide with the symmetry axes of the crystal and are close to real [7]. The influence of the first term in formula (4) causes \mathbf{M}_{Fe} to slightly deviate from the $[210]$ axis to the $[110]$. As the temperature rises in the $[uv0]$ phase, the vector \mathbf{M}_{Fe} moves in the (001) plane from the $[210]$ axis to the $[110]$ axis, then at intermediate temperatures $T_2 < T < T_1$ the phase $[110]$ is realized, and then at high temperatures $T > T_1$ — phase $[111]$ (see Fig. 1).

The configurations of the \mathbf{M}_k magnetic moments of the Sm^{3+} ions in all three phases listed are shown in Figs 2, 3, 4.

4. Electric dipole moments of samarium ions induced by exchange field

It was shown in [4] that the contribution of an individual rare-earth ion with a doublet (or quasi-doublet) ground state to the magneto electric energy $\mathcal{E}_{\text{me}}^{(k)}$ of a crystal with a garnet structure is combinations of products of the components of the vectors \mathbf{E} , \mathbf{H} , and \mathbf{M} that are invariant under transformations of the D_2 group. In case of samarium ions in ferrite garnet at low temperatures $T < E_1/k \sim 120$ K, when one can limit oneself to populating the levels of the main doublet, in the local axes of the k -th place,

$$\mathcal{E}_{\text{me}}^{(k)} = C_1 M_x^{(k)} H_y^{(k)} E_z^{(k)} + C_2 M_x^{(k)} H_z^{(k)} E_y^{(k)}, \quad (5)$$

where $\mathbf{H} = \mathbf{H}_{\text{eff}} = \lambda \mathbf{M}_{\text{Fe}}$ and $M_x^{(k)}$ defined by expression (2). Dipole moment of an ion at k -th place

$$P_\alpha^{(k)} = -\frac{\partial \phi_{\text{me}}^{(k)}}{\partial E_\alpha^{(k)}}, \quad \alpha = x, y, z. \quad (6)$$

It suffices for us to consider the induction of electric dipole moments at the first six sites of rare-earth ions in the cell. The dipole moments of the remaining places are found using the relations $P_\alpha^{(k+6)} = -P_\alpha^{(k)}$, which are valid for even magnetic structures and in the case of a homogeneous magnetic (exchange) field. Consider in turn the phases [1 1 1], [1 1 0] and [u v 0].

For the low-temperature phase [u v 0] let us find

$$\mathbf{P}^{(1,2)} = \pm \frac{\mu H_{\text{eff}}}{\sqrt{2}} \text{th} \left(\frac{\gamma_x \pm \gamma_y}{\tau \sqrt{2}} \right) C_1 (\gamma_x \mp \gamma_y) \mathbf{e}_z,$$

$$\mathbf{P}^{(3,4)} = \pm \frac{\mu H_{\text{eff}}}{\sqrt{2}} \text{th} \left(\frac{\gamma_y}{\tau \sqrt{2}} \right) (C_1 \gamma_y \mathbf{e}_x + C_2 \gamma_x (\mathbf{e}_y \mp \mathbf{e}_z)),$$

$$\mathbf{P}^{(5,6)} = \mp \frac{\mu H_{\text{eff}}}{\sqrt{2}} \text{th} \left(\frac{\gamma_x}{\tau \sqrt{2}} \right) (C_1 \gamma_x \mathbf{e}_y + C_2 \gamma_y (\mathbf{e}_x \mp \mathbf{e}_z)), \quad (7)$$

where $\tau = kT/\mu H_{\text{eff}}$, $\mathbf{e}_x = [1 0 0]$, $\mathbf{e}_y = [0 1 0]$, $\mathbf{e}_z = [0 0 1]$,

$$\gamma_x = \frac{u(\tau)}{\sqrt{u^2(\tau) + v^2(\tau)}} \quad \text{and} \quad \gamma_y = \frac{v(\tau)}{\sqrt{u^2(\tau) + v^2(\tau)}}.$$

It suffices to set $\gamma_x = \gamma_y = 1/\sqrt{2}$ for the phase [1 1 0] in equations (7).

The simplest configuration of electric dipole and magnetic moments is realized in the case of the high-temperature phase [1 1 1], in which (see Fig. 5)

$$\mathbf{P}^{(2)} = \mathbf{P}^{(4)} = \mathbf{P}^{(6)} = 0,$$

$$\mathbf{P}^{(1)} = C_2 \frac{\mu H_{\text{eff}}}{\sqrt{6}} \text{th} \left(\frac{\sqrt{6}}{3\tau} \right) (\mathbf{e}_x - \mathbf{e}_y),$$

$$\mathbf{P}^{(3)} = C_2 \frac{\mu H_{\text{eff}}}{\sqrt{6}} \text{th} \left(\frac{\sqrt{6}}{3\tau} \right) (\mathbf{e}_y - \mathbf{e}_z),$$

$$\mathbf{P}^{(5)} = C_2 \frac{\mu H_{\text{eff}}}{\sqrt{6}} \text{th} \left(\frac{\sqrt{6}}{3\tau} \right) (\mathbf{e}_z - \mathbf{e}_x). \quad (8)$$

Let us note that in all three phases the vectors $\mathbf{P}^{(k)}$ and $\mathbf{M}^{(k)}$ are perpendicular to each other. As for the resulting polarization vector $\sum_{k=1}^6 \mathbf{P}^{(k)}$, then the phases [u v 0] and [1 1 0] it is nonzero and is directed along the [0 0 1] axis. In phase [1 1 1] the vectors $\mathbf{P}^{(1,3,5)}$ are perpendicular to the axes [1 1 1] and $\sum_{k=1}^6 \mathbf{P}^{(k)} = 0$. It is inevitably, in the case of a uniform exchange field, the resulting electric dipole moment of the lattice cell $\sum_{k=1}^{24} \mathbf{P}^{(k)}$ vanishes due to the relations $P_\alpha^{(k+6)} = -P_\alpha^{(k)}$. The occurrence of polarization in the subsystem of rare-earth ions in iron garnets is possible in the case of a heterogeneous exchange field, which is realized, in particular, in the zone of domain walls.

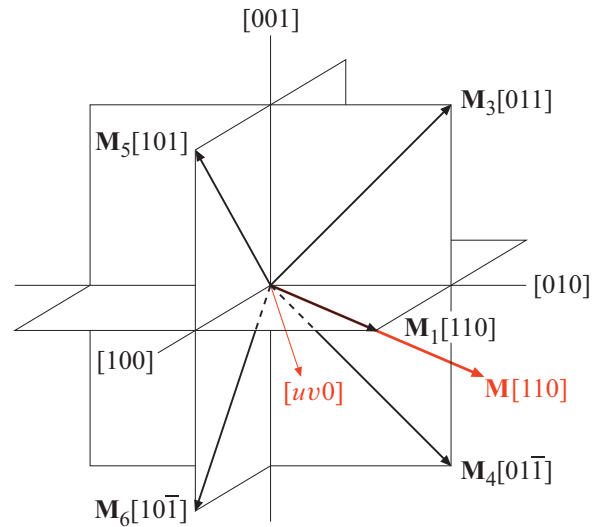


Figure 3. Configuration of magnetic moments of samarium ions in the [1 1 0] phase, in which $\mathbf{M}_2 = 0$, which is realized at $T_2 < T < T_1$.

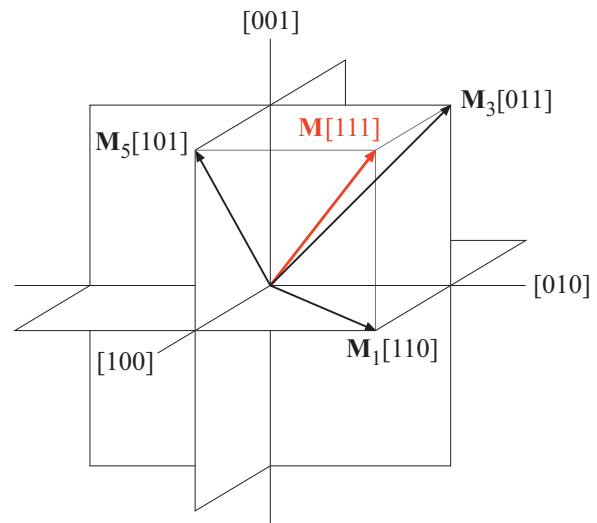


Figure 4. Configuration of magnetic moments of samarium ions in the [1 1 1] phase, which is realized at temperatures $T > 65.7$ K. In this phase $\mathbf{M}_2 = \mathbf{M}_4 = \mathbf{M}_6 = 0$.

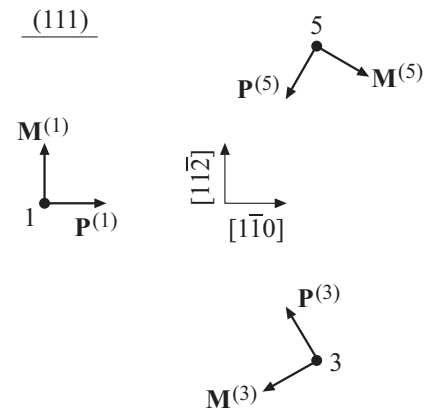


Figure 5. Configuration of electric and magnetic dipole moments of samarium ions in the projection onto the (1 1 1) plane for the [1 1 1] phase realized at temperatures $T > T_1 = 65.7$ K.

5. Polarization of domain walls in SmIG

The polarization of the subsystem of rare-earth ions in domain walls, due to the inhomogeneity of the exchange field acting on rare-earth ions, was studied in works [5,12,13]. In these works, ordinary Bloch-type domain walls were reviewed, in which the vector \mathbf{M}_{Fe} was rotated through an angle 71° from the direction $[111]$ to the $[11\bar{1}]$ direction along the $[\bar{1}10]$ axis, as well as Neel-type domain boundaries, in which the vector \mathbf{M}_{Fe} is rotated from the $[\bar{1}\bar{1}\bar{1}]$ axis to $[111]$ axes.

Let us note that in the indicated works [5,12,13] the electric dipole moment of the primitive cell doubled was taken as the polarization, while in such cases the lattice cell should be used [6]. Therefore, in this work, we will study below the polarization of the Bloch domain wall, which arises, in particular, in SmIG at a temperature $T > T_1 = 65.7\text{K}$, taking into account the indicated circumstance, and also study the polarization of SmIG domain walls, which are realized at low temperatures ($T \rightarrow 0\text{K}$).

The uniqueness of SmIG lies in the fact that at low temperatures the easy magnetization axes are $[uv0]$ directions, which do not coincide with the symmetry axes of the cubic crystal. In the limit $T \rightarrow 0\text{K}$, these directions are close to $\langle 210 \rangle$, so here Bloch walls will be realized, in which \mathbf{M}_{Fe} rotates through the angle 37° from the direction $[210]$ to the direction $[120]$, or through the angle 66° when turning from $[210]$ to $[021]$, or by 78° in case of turning from $[210]$ to $[012]$.

Let us consider the polarization of the lowest energy 37° -degree domain wall. Let the vector \mathbf{M}_{Fe} rotate along the axis $z = [001]$ from the direction $[210]$ to direction $[120]$. The anisotropy energy density of samarium ferrite garnet at $T \rightarrow 0\text{K}$ can be represented as $E_A = nE_1$, where, according to (4), the expression

$$E_1 = -\frac{1}{6} \mu_x \lambda M_{\text{Fe}} \sum_{k=1}^6 |\mathbf{m} \cdot \mathbf{e}_x^{(k)}|$$

is the thermodynamic potential of the system per one samarium ion due to the splitting of the main doublet Sm^{3+} in the effective exchange field, $n = 24/d^3$ is the number of samarium ions per unit volume, and $d \sim 1.2\text{nm}$ — lattice cell edge length. Thus,

$$E_A = -K \sum_{k=1}^6 |\mathbf{m} \cdot \mathbf{e}_x^{(k)}|, \quad (9)$$

where $K = 4\mu_x \lambda M_{\text{Fe}}/d^3$. Let us represent the vector \mathbf{m} in the form

$$\mathbf{m} = \mathbf{e}_x \cos\left(\varphi + \frac{\pi}{4}\right) + \mathbf{e}_y \sin\left(\varphi + \frac{\pi}{4}\right), \quad (10)$$

where the angle φ is measured from axis $[110]$, and $\mathbf{e}_x = [100]$ and $\mathbf{e}_y = [010]$. In this case, the terms included

in the sum in expression (9) have the form

$$\begin{aligned} (\mathbf{m} \cdot \mathbf{e}_x^{(1)}) &= \frac{1}{\sqrt{2}} \cos\left(\varphi + \frac{\pi}{4}\right) + \frac{1}{\sqrt{2}} \sin\left(\varphi + \frac{\pi}{4}\right) \\ &= \cos \varphi, \end{aligned}$$

$$\begin{aligned} (\mathbf{m} \cdot \mathbf{e}_x^{(2)}) &= \frac{1}{\sqrt{2}} \cos\left(\varphi + \frac{\pi}{4}\right) - \frac{1}{\sqrt{2}} \sin\left(\varphi + \frac{\pi}{4}\right) \\ &= -\sin \varphi, \end{aligned}$$

$$(\mathbf{m} \cdot \mathbf{e}_x^{(3,4)}) = \frac{1}{\sqrt{2}} \sin\left(\varphi + \frac{\pi}{4}\right),$$

$$(\mathbf{m} \cdot \mathbf{e}_x^{(5,6)}) = \pm \frac{1}{\sqrt{2}} \cos\left(\varphi + \frac{\pi}{4}\right).$$

Thus we obtain

$$E_A = -K(3 \cos \varphi + |\sin \varphi|) = -K\sqrt{10} \cos\left(\frac{\varphi_0}{2} - |\varphi|\right),$$

where $\varphi_0 = \arccos(4/5) = 37^\circ$ — angle between the axes $[210]$ and $[120]$.

The Euler–Lagrange equation for such E_A has the form

$$A \left(\frac{\partial \varphi}{\partial z}\right)^2 = K\sqrt{10} \left(1 - \cos\left(\frac{\varphi_0}{2} - |\varphi|\right)\right), \quad (11)$$

where $A \sim 10^{-7}\text{erg/cm}$ — is the heterogeneous exchange constant. Separation of variables in the differential equation (11) leads to the integral

$$z \cdot 10^{1/4} \sqrt{\frac{K}{A}} = \int \frac{d\varphi}{\sqrt{1 - \cos\left(\frac{\varphi_0}{2} - |\varphi|\right)}},$$

whence we find the expression that determines the shape of the domain wall

$$\text{tg}\left(\frac{\varphi_0}{8} - \frac{\varphi}{4}\right) = \text{tg}\left(\frac{\varphi_0}{8}\right) \cdot \exp\left(\pm \frac{z}{z_0}\right), \quad (12)$$

where the quantity z_0 is given by the relation

$$z_0 = 10^{-1/4} \sqrt{\frac{A}{2K}}. \quad (13)$$

In the formula (12), the upper sign corresponds to $z < 0$ and $\varphi < 0$, and the lower — to $z > 0$ and $\varphi > 0$. Since the angles $\varphi_0/8$ and $\varphi_0/8 \pm \varphi/4$ are very small (less than 5°), equation (12) can be represented as

$$\varphi(z) = \mp \frac{\varphi_0}{2} (1 - e^{\pm z/z_0}), \quad (14)$$

where again the upper sign should be used for $z < 0$, and the lower — for $z > 0$.

The domain wall polarization vector is defined as the electric dipole moment of samarium ions in a lattice cell located at a given point, related to the volume of the cell.

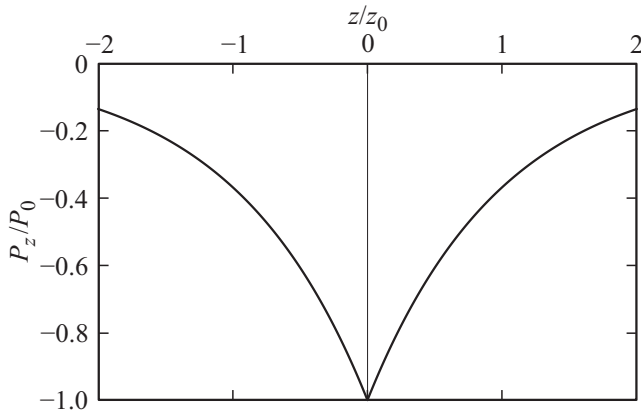


Figure 6. Dependence of the electric polarization $P(z)$ of the Bloch domain wall, in which the magnetization vector \mathbf{M}_{Fe} turns from the direction $[210]$ to the direction $[120]$ along the $[001]$ axis, from the z coordinate (in relative units). The values z_0 and P_0 are given by relations (13) and (15), respectively.

According to relations (6), the electric dipole moments of samarium ions are equal

$$\mathbf{P}^{(k)} = -C_1 M_x^{(k)} H_y^{(k)} \mathbf{e}_z^{(k)} - C_2 M_x^{(k)} H_z^{(k)} \mathbf{e}_y^{(k)},$$

where $\mathbf{H} = \lambda \mathbf{M}_{\text{Fe}} = \lambda M_{\text{Fe}} \mathbf{m}$. In turn, at a temperature $T \rightarrow 0 \text{ K}$, the magnetic dipole moments of samarium ions are $M_x^{(k)} = \mu_x \text{sign}(\mathbf{m} \cdot \mathbf{e}_x^{(k)})$ are $M_x^{(1,3,4,5)} = \mu_x$, $M_x^{(6)} = -\mu_x$, $M_x^{(2)} = -\mu_x \text{sign} z$, according to formula (10) defining the vector \mathbf{m} .

Let us use the relation

$$f(\mathbf{r}_k) - f(\mathbf{r}_{k+6}) = (\nabla f)(\mathbf{r}_k - \mathbf{r}_{k+6})$$

and find that

$$\sum_{i=k}^{24} \mathbf{P}^{(k)} = -\frac{1}{2} C_1 \mu_x \lambda M_{\text{Fe}} d (\cos \varphi(z) - |\sin \varphi(z)|) \frac{\partial \varphi(z)}{\partial z} \mathbf{e}_z.$$

Let us divide this expression by the volume d^3 of the lattice cell and find the polarization vector

$$\mathbf{P} = -\frac{C_1 \mu_x \lambda M_{\text{Fe}}}{d^2} (\cos \varphi(z) - |\sin \varphi(z)|) \frac{\partial \varphi(z)}{\partial z} \mathbf{e}_z,$$

directed along the magnetization reversal axis (z axis). According to formula (14), the angle $\varphi \ll 1$, while the expression for the vector $\mathbf{P}(z)$ takes the simple form

$$\mathbf{P}(z) = -P_0 e^{-\frac{|z|}{z_0}} \mathbf{e}_z, \quad P_0 = \frac{C_1 \mu_x \lambda M_{\text{Fe}}}{d^2} \frac{\varphi_0}{2z_0}. \quad (15)$$

The dependence $P(z)$ is shown in Fig. 6.

Let us now consider the electric polarization of the Bloch domain wall, which is realized at a temperature $T > T_1$, in which the vector \mathbf{M}_{Fe} rotates through an angle 71° from

the direction $[111]$ to the direction $[11\bar{1}]$ along the axis $\tilde{z} \parallel [\bar{1}10]$. In this case

$$\mathbf{m} = \frac{\mathbf{M}_{\text{Fe}}}{M_{\text{Fe}}} = \mathbf{e}_{\tilde{x}} \cos \varphi + \mathbf{e}_{\tilde{y}} \sin \varphi,$$

where φ — is the angle defining the orientation of the magnetization vector \mathbf{M}_{Fe} in the laboratory coordinate system $\mathbf{e}_{\tilde{x}} = [111]$, $\mathbf{e}_{\tilde{y}} = [11\bar{2}]$, $\mathbf{e}_{\tilde{z}} = [\bar{1}10]$. The distribution of magnetization in the Bloch domain wall is determined by the relations given in work [14]:

$$\frac{\partial \varphi}{\partial \tilde{z}} = \sqrt{\frac{K_1}{A}} \left(\frac{1}{2} \cos^4(\gamma - \varphi) + \sin^4(\gamma - \varphi) - \frac{1}{3} \right)^{1/2}, \quad (16)$$

$$\varphi(\tilde{z}) = \gamma + \text{arctg} \left(\frac{1}{\sqrt{2}} \text{th} \left(\tilde{z} \sqrt{\frac{K_1}{3A}} \right) \right),$$

where A — is the heterogeneous exchange interaction constant, K_1 — is the absolute value of the magnetic anisotropy constant, and $2\gamma = 2 \text{arctg}(1/\sqrt{2}) = 71^\circ$ — angle of complete rotation of the magnetization vector in the domain wall.

At a temperature $T > T_1 = 65.7 \text{ K}$, according to [10], the splitting of Sm^{3+} doublets in the exchange interaction field is less than kT , and in this case the electric dipole moments of Sm^{3+} ions (as well as other RE-ions), according to [5], take the form

$$\mathbf{P}^{(k)} = -d_1 \mathbf{e}_x^{(k)} m_y^{(k)} m_z^{(k)} - d_2 \mathbf{e}_y^{(k)} m_x^{(k)} m_z^{(k)} - d_3 \mathbf{e}_z^{(k)} m_x^{(k)} m_y^{(k)},$$

where d_i ($i = 1, 2, 3$) — constants determined by wave functions and energy levels of rare-earth ions in the crystal field, as well as temperature (see work [5]).

Next, it is required to sum the vectors $\mathbf{P}^{(k)}$ over all 24 samarium ions in the lattice cell, and then divide by the volume of the cell d^3 and thereby obtain the polarization $P(\tilde{z})$. Since $\mathbf{e}_\alpha^{(k+6)} = -\mathbf{e}_\alpha^{(k)}$, the sum $\sum_{k=1}^{24}$ will contain the differences $f(\mathbf{r}_k) - f(\mathbf{r}_{k+6})$, where f — trigonometric functions.

In the case we are considering $f(\mathbf{r}_k) = f(\varphi(\mathbf{r}_k))$, and the angle φ , in turn, is $\varphi(\tilde{z})$, so

$$f(\mathbf{r}_k) - f(\mathbf{r}_{k+6}) = \frac{\partial f(\varphi)}{\partial \varphi} \frac{\partial \varphi(\tilde{z})}{\partial \tilde{z}} (\mathbf{e}_{\tilde{z}} \cdot (\mathbf{r}_k - \mathbf{r}_{k+6})).$$

Let us use this relation and find that the electric polarization vector of the 71-degree domain wall

$$\begin{aligned} \mathbf{P} &= \frac{1}{d^3} \sum_{k=1}^{24} \mathbf{P}^{(k)} = (q_1 \Phi_1(\tilde{z}) + q_2 \Phi_2(\tilde{z})) \mathbf{e}_{\tilde{x}} \\ &+ \frac{1}{\sqrt{2}} (q_1 \Phi_1(\tilde{z}) + \sqrt{3} q_2 \Phi_3(\tilde{z})) \mathbf{e}_{\tilde{y}}. \end{aligned} \quad (17)$$

The following notations are introduced here

$$q_1 = \frac{\sqrt{3}}{4} \frac{d_3}{d^2} \quad \text{and} \quad q_2 = \frac{\sqrt{2}}{4} \frac{d_1 + d_2}{d^2},$$

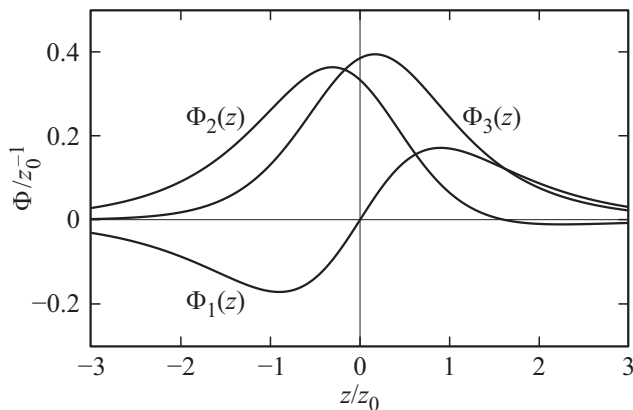


Figure 7. Dependences $\Phi_1(z)$, $\Phi_2(z)$ and $\Phi_3(z)$ given by formulas (18) and (16), in relative units. Value of z_0 is defined by expression (13).

as well as

$$\begin{aligned}\Phi_1(\tilde{z}) &= \frac{\partial\varphi(\tilde{z})}{\partial\tilde{z}} \sin(2\varphi(\tilde{z}) - 2\gamma), \\ \Phi_2(\tilde{z}) &= \frac{\partial\varphi(\tilde{z})}{\partial\tilde{z}} \cos(2\varphi(\tilde{z}) - \gamma), \\ \Phi_3(\tilde{z}) &= \frac{\partial\varphi(\tilde{z})}{\partial\tilde{z}} \sin(2\varphi(\tilde{z})),\end{aligned}\quad (18)$$

where the values $\varphi(\tilde{z})$ and $\partial\varphi(\tilde{z})/\partial\tilde{z}$ are defined by relations (16). Let us note that in this case the wall polarization vector is oriented perpendicular to the turn axis, i.e., $\mathbf{P} \perp \mathbf{e}_{\tilde{z}}$. Graphs of functions $\Phi_{1,2,3}(\tilde{z})$ are shown in Fig. 7.

6. Conclusion

This work was mainly aimed at revealing the magneto electric properties of samarium ferrite garnet, which has unique magnetic characteristics. The configurations of electric dipole moments of samarium ions induced by the field of exchange R-Fe interactions were determined, and the connection with magnetic structures and their transformations during orientational magnetic phase transitions was revealed.

The opportunity of realizing at low temperatures $T \rightarrow 0$ K unusual 37° Bloch domain walls is specified, in which the magnetization vector of the iron ion sublattices \mathbf{M}_{Fe} is rotated, from $[210]$ -type axes to $[120]$ axes and their quantitative description is carried out. The electric polarization of such Bloch boundaries is calculated.

The electric polarization of the 71° -x domain walls that arise in SmIG at high temperatures $T > T_1 = 65.7$ K, where \mathbf{M}_{Fe} expands from $[111]$ axes to $[11\bar{1}]$ axes. The results obtained in this case are applicable not only to SmIG, but also to most other rare-earth ferrite garnets, whose easy magnetization axes are $[111]$ directions.

It has been established that the electric polarization of Bloch domain walls, which arises as a result of the

heterogeneous magneto electric effect, depends significantly on the shape of the boundaries. So in case of the 37° -degree boundary, where the rotation of the vector \mathbf{M}_{Fe} occurs from the axis $[210]$ to the axis $[120]$ along the vector $[001]$ the polarization \mathbf{P} is directed along the axis of rotation, and for 71° -degree boundary of the domain boundary, in which the vector \mathbf{M}_{Fe} unfolds from the direction $[111]$ to $[11\bar{1}]$ along the $\tilde{z} \parallel [\bar{1}10]$ axis, the polarization vector is perpendicular to the turn axis.

Funding

This work was supported by the Strategic Academic Leadership Program of the Peoples' Friendship University of Russia (PFUR). AKZ is grateful to the Russian Science Foundation for supporting this work (project of the Russian Science Foundation No. 22-12-00367).

Conflict of interest

The authors declare that they have no conflict of interest.

References

- [1] N.A. Spaldin, R. Ramesh. *Nature Mater.* **18**, 202 (2019). <https://doi.org/10.1038/s41563-018-0275-2>
- [2] X. Liang, H. Chen, N.X. Suna. *Appl. Phys. Lett. Mater.* **9**, 041114 (2021). <https://doi.org/10.1063/5.0044532>
- [3] A.K. Zvezdin, A.A. Mukhin. *Pis'ma v ZhETF* **88**, 8, 581 (2008). (in Russian). http://jetpletters.ru/ps/1852/article_28266.shtml
- [4] A.I. Popov, D.I. Plokhov, A.K. Zvezdin. *Phys. Rev. B* **90**, 214427 (2014). <https://doi.org/10.1103/PhysRevB.90.214427>
- [5] A.I. Popov, Z.V. Gareeva, A.K. Zvezdin. *Phys. Rev. B* **92**, 144420 (2015). <https://doi.org/10.1103/PhysRevB.92.144420>
- [6] A.I. Popov, Ch.K. Sabdenov. *FTT* **61**, 6, 1084 (2019). (in Russian). <https://doi.org/10.21883/FTT.2019.06.47682.351>
- [7] G.A. Babushkin, V.A. Borodin, V.D. Doroshev, A.K. Zvezdin, R.Z. Levitin, A.I. Popov. *Pis'ma v ZhETF* **35**, 1, 28 (1982). (in Russian). http://jetpletters.ru/ps/358/article_5642.shtml
- [8] A.K. Zvezdin, V.M. Matveev, A.A. Mukhin, A.I. Popov. *Redkozemelnyye iony v magnitouporyadochennykh kristallakh*. Nauka, M. (1985). 296 p. (in Russian).
- [9] O.A. Dorofeev, A.I. Popov. *FNT* **32**, 11, 3425 (1990). (in Russian). <http://journals.ioffe.ru/articles/21435>
- [10] O.A. Dorofeev, A.I. Popov. *FTN* **31**, 11, 124 (1989). (in Russian). <http://journals.ioffe.ru/articles/28969>
- [11] A.K. Zvezdin, A.A. Mukhin, A.I. Popov. *Pisma v ZhETF* **23**, 5, 267 (1976). http://jetpletters.ru/ps/571/article_8976.shtml
- [12] A.I. Popov, K.A. Zvezdin, Z.V. Gareeva, F.A. Mazhitova, R.M. Vakhitov, A.R. Yumaguzin, A.K. Zvezdin. *J. Phys.: Condens. Matter* **28**, 456004 (2016). <https://doi.org/10.1088/0953-8984/28/45/456004>
- [13] A.I. Popov, Z.V. Gareeva, A.K. Zvezdin, T.T. Gareev, A.S. Sergeev, A.P. Pyatakov. *Ferroelectrics* **509**, 32 (2017). <https://doi.org/10.1080/00150193.2017.1292111>
- [14] A.M. Alekseev, A.F. Popkov, A.I. Popov. *FTT* **41**, 12, 2183 (1999). <https://journals.ioffe.ru/articles/35642>

Translated by E.Potapova